

Chapter 16

External Strengthening of Continuous RC Beams with CFRP

Pieter Desnerck, Lander Vasseur, Stijn Matthys, and Luc Taerwe

Abstract The structural behaviour of reinforced beams strengthened in flexure with externally bonded FRP (Fibre Reinforced Polymer) reinforcement has been extensively investigated with respect to isostatic beams. Design methods are given in guidelines and standards, and failure modes are described. However, limited information is available on the behaviour of continuous beams, strengthened with composite reinforcement. For flexural strengthening of a 2-span continuous beam, the FRP reinforcement can be applied on top of the central support, at the bottom-side of the two spans or at both locations. By means of an analytical study, the non-linear behaviour of this type of beam is investigated. The failure modes are studied and it is verified to which degree moment redistribution is still present when applying this strengthening technique which makes use of a linear elastic polymeric material.

16.1 Introduction

Structures may need to be strengthened for different reasons, among which is a change in function, the implementation of additional services, or the repair of damage. Different strengthening techniques are possible, but often used nowadays is the application of an externally bonded reinforcement (EBR) consisting of a fibre-reinforced polymer (FRP), the so-called FRP EBR. FRP ('Fibre Reinforced Polymer')

P. Desnerck (✉) • S. Matthys • L. Taerwe
Department of Structural Engineering, Magnel Laboratory for Concrete Research,
Ghent University, Technologiepark-Zwijnaarde 904, B-9052 Zwijnaarde, Belgium
e-mail: pieter.desnerck@ugent.be; stijn.matthys@ugent.be; luc.taerwe@ugent.be

L. Vasseur
ECC NV Belgium, Terbekehofdreef 50-52, B-2610 Antwerp, Belgium
e-mail: lander.vasseur@ecc-belgium.be

or ‘Fibre Reinforced Plastic’) is a composite material consisting of non-metallic fibres imbedded in a polymeric matrix. Generally a thermoset material such as polyester, vinyl ester or epoxy resin is used as matrix. The types of fibres mostly applied for civil constructions are: glass fibres (GFRP), aramid fibres (AFRP) and carbon fibres (CFRP), the latter type being used in this study.

FRP EBR can be used for the strengthening of existing structures in order to enhance their flexural and shear capacity. This paper discusses the flexural strengthening of 2-span reinforced concrete beams. CFRP (Carbon FRP) laminates are glued on the soffit of spans and/or on the top at the mid-support (Nanni 1993; NBN-EN-1504-5 2005). Besides the more regular failure modes of beams in flexure (concrete crushing, rebar yielding, etc.), the efficiency of the FRP EBR strengthening technique is limited by the capability to transfer stresses at the bond interface. Often debonding of the laminate will lead to overall failure of the element. Hence, the aim of this study is to gain a better insight into the behaviour and failure mode of reinforced multispan concrete beams strengthened in flexure with CFRP.

16.2 Moment Redistribution

Performing an analysis of a structure according to the linear elastic theory, a linear relationship between the moment and the curvature is assumed, i.e.

$$\chi = \frac{1}{r} = \frac{M}{EI} \tag{16.1}$$

with $1/r$ the curvature, M the bending moment and $EI=K$ the flexural rigidity, which is often assumed to be constant and therefore independent of the value of the bending moment. However, for the cross-section of a concrete beam the moment-curvature diagram is non-linear, which corresponds to a variable flexural rigidity. This is illustrated in Fig. 16.1, where the non-linear behaviour is simplified by three straight branches each characterized by a specific flexural rigidity.

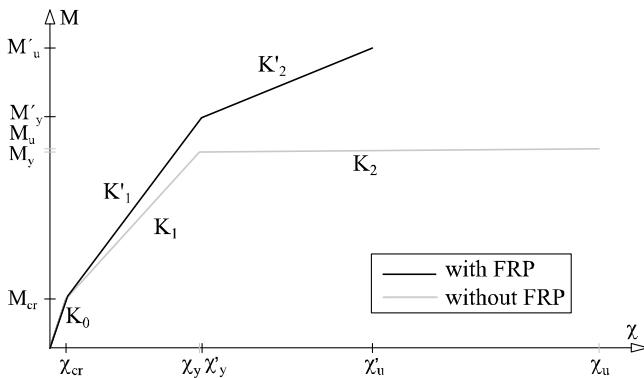


Fig. 16.1 Moment-curvature diagram: influence of flexural strengthening

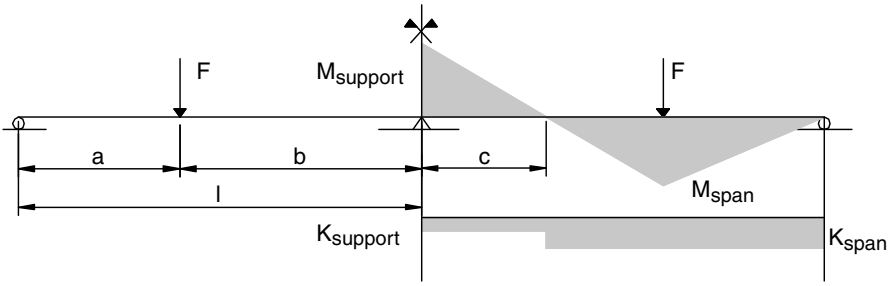


Fig. 16.2 Two-span beam with stepwise constant flexural rigidity

Figure 16.1 compares the $M-\chi$ relationship of an unstrengthened and an FRP flexural strengthened RC cross-section. K_0 represents the flexural rigidity of the uncracked concrete section, K_1 of the section after cracking and K_2 of the cracked section after yielding of the steel reinforcement. In a cross-section with both steel and externally bonded FRP reinforcement, higher values of K (especially K_2 and K'_2) are obtained in comparison with the same beam without FRP. Due to strengthening a higher bending moment capacity is obtained whereas the ultimate curvature is reduced. This different behaviour will influence the moment redistribution of a continuous beam.

Considering a continuous beam with two identical spans and two symmetric point loads (Fig. 16.2), three zones can be identified:

- The central mid-support zone with hogging moments.
- The span zones with sagging moments.

It is assumed that in each zone, the flexural rigidity is constant. The flexural rigidity of the mid-support zone and the span zones is designated respectively as $K_{support}$ and K_{span} . Referring to Fig. 16.2, the non-dimensional variables m (moment ratio), k (flexural rigidity ratio) and λ (location of point loads) are introduced:

$$m = \frac{M_{support}}{M_{span}} \quad k = \frac{K_{support}}{K_{span}} \quad \lambda = \frac{a}{b} \tag{16.2}$$

Using equilibrium equations, requiring the rotation above the mid-support to be zero and fixing λ to $2/3$ (see tests discussed in Sect. 16.4), the following relationship between the two basic variables can be derived:

$$36m^3 + (45 - 8k)m^3 - 34km - 35k = 0 \tag{16.3}$$

Given the $k-m$ relationship which is valid for the specific beam geometry and loading configuration, the bending moment ratio m can be derived from the known flexural rigidity ratio k , which depends on the internal and the external reinforcement ratios and on the load level.

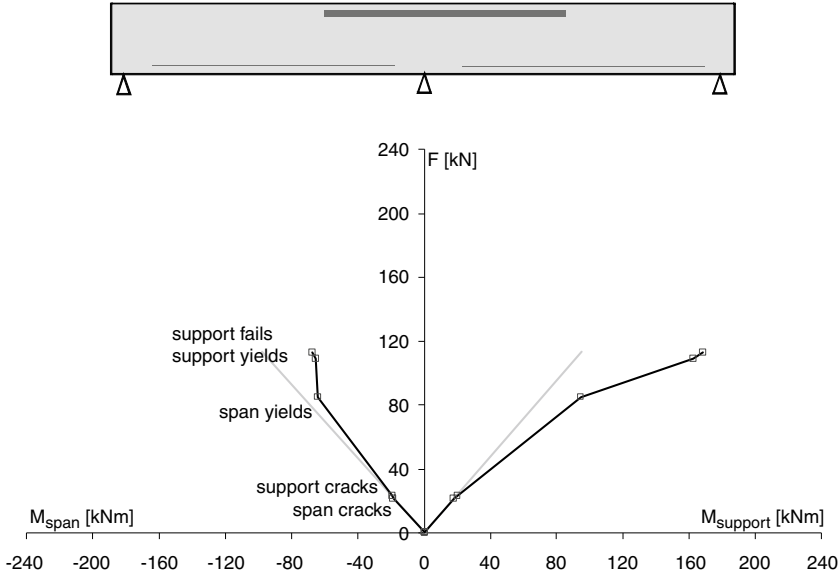


Fig. 16.3 Redistribution graphs for unstrengthened 2-span beam

In Fig. 16.3 a comparison is made between a strengthened and an unstrengthened 2-span beam with a equal to 2 m and b equal to 3 m. The span and support moments are plotted as a function of the loads F . The span section being the most critical, the first plastic hinges occur in the spans. All additional loading is taken by the mid-support (Fig. 16.3). By using FRP EBR at both locations (Fig. 16.4), it is noticed that after yielding of both critical cross-sections the moment distribution is parallel to the linear elastic moment distribution.

A comparable situation is seen when the reinforcement in the spans of the beam is increased and the first plastic hinge is formed at the mid-support. Applying FRP EBR at the top of the beam at the mid-support allows for the suppression of the formation of a plastic hinge at that location and the bending moments are closer to the elastic curve. The theoretically obtained redistribution curves show a good to excellent agreement with the experimentally obtained moment redistribution (see Sect. 16.4).

16.3 Debonding Mechanisms

For the design of an externally strengthened beam at the ultimate limit state (ULS), guidelines recommend a two stage analysis (fib 2001; Matthys 2000; ACI 2002). First, the strengthened beam is designed assuming a full composite action (meaning

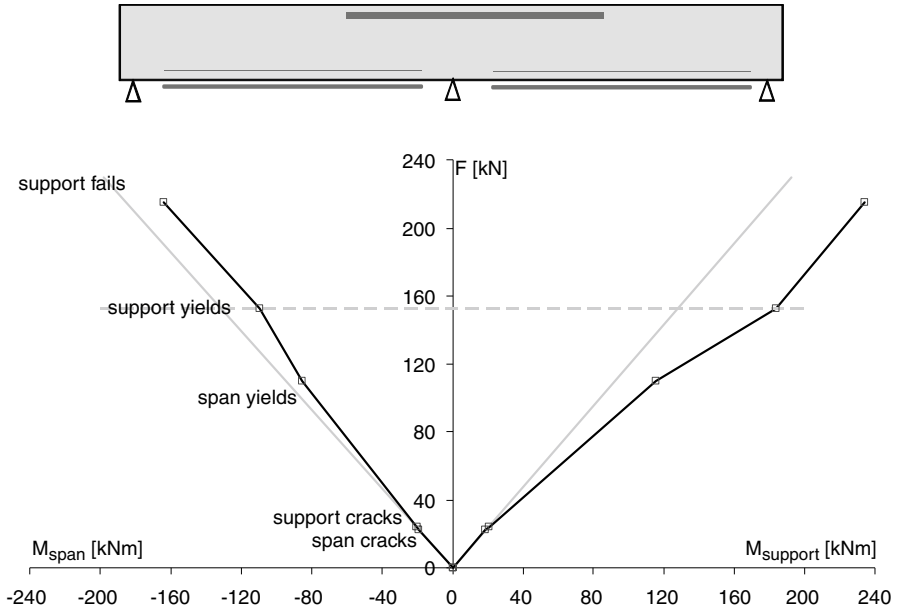


Fig. 16.4 Redistribution graphs for FRP EBR strengthened 2-span beam

no debonding of the FRP EBR material from the concrete is taken into account). One of the following failure modes occurs:

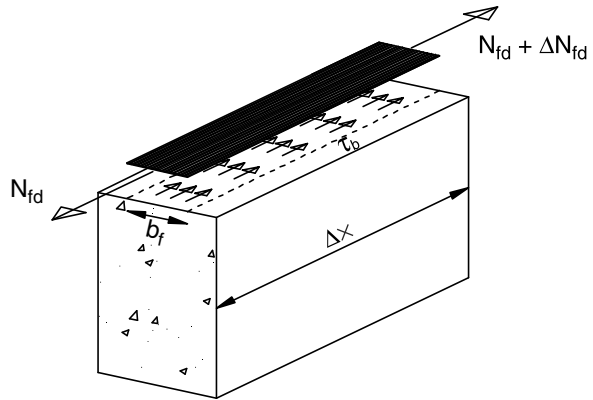
- Steel yielding followed by concrete crushing
- Steel yielding followed by FRP fracture
- Concrete crushing without steel yielding.

In the second design stage of an externally strengthened beam at the ultimate limit state (ULS), the loss of composite action between the concrete and the FRP reinforcement has to be checked. This type of failure typically occurs in a sudden and brittle way.

In practice, debonding in the adhesive or FRP is generally not noticed because the tensile and shear strength of the resin or adhesive are mostly higher than that of the concrete. Hence, it can be concluded that debonding normally occurs in the concrete, near to the surface or along the embedded reinforcement. The exact location of debonding in the concrete cover is dependent on the type of debonding mechanism which is typical for a certain type of beam and strengthening configuration. According to *fib* Bulletin 14 (2001) and Matthys (2000) different bond failure types can be distinguished, i.e.:

- Debonding at flexural cracks (crack bridging)
- Debonding at shear cracks (crack bridging)
- Curtailment or anchorage length failure
- End shear failure.

Fig. 16.5 Shear stresses along FRP laminate element



16.3.1 Crack Bridging

For the debonding phenomena by crack bridging, a distinction is made between the bridging of flexural cracks and the bridging of shear cracks by the FRP laminate.

Flexural cracks are characterized by a horizontal crack opening. At both sides of a crack, high peak shear stresses occur. When the peak shear stress exceeds the maximum shear stress $\tau_{b,max}$, a gradual debonding is noticed, initiated by micro-cracking and finally continuing in macro-cracking.

When debonding is initiated, the shear stress redistributes and a smoothing effect occurs for the ideal case of pure flexure. From this smoothing of the shear stresses, one could conclude that this debonding failure mode is less critical than crack bridging at flexural cracks in regions with additional shear forces and hence vertical crack displacement (Matthys 2000). As indicated by several authors (Teng et al. 2003; Oller et al. 2007; Chen et al. 2007), debonding at the location of a flexural crack can result in a complete debonding of the FRP laminate and has to be checked consequently. According to *fib* Bulletin 14 (2001), checking of peeling off failure at flexural cracks can be performed according to several approaches.

One of these methods is the verification of the bond stresses due to force transfer. The variation of the tensile force in the FRP initiates bond shear stresses τ_b at the interface. To avoid debonding of the laminate by this mechanism, the shear stress between the FRP and the concrete, resulting from the change of tensile force along the length of the laminate, has to be limited. This shear stress is calculated as follows, based on the equilibrium of forces as can be seen in Fig. 16.5 and assuming a uniform bond stress over the distance Δx .

$$\tau_b = \frac{\Delta N_{fd}}{b_f \Delta x} \quad (16.4)$$

In the ULS, this acting shear stress has to be limited to the design bond shear strength f_{cbd} , which is given by the following equation:

$$f_{cbd} = 1.8 \frac{f_{ctk}}{\gamma_c} \quad (16.5)$$

When the width of the bond interface b_f is sufficient, this limitation of the shear stress will not be critical in most cases. However, in case the internal steel reinforcement is yielding, the increase in tensile force under increasing bending moment is uniquely provided by the FRP laminate resulting in higher values of ΔN_{fd} and τ_b . In this case debonding may become critical.

In regions with significant shear forces, the shear cracks are inclined, and are associated with both horizontal and vertical crack displacements. Crack bridging models for shear cracks explicitly consider the combined effect of horizontal and vertical displacements. Due to the horizontal crack displacement, peak shear stresses are induced. On the other hand, the vertical crack displacement results in an additional peeling-off effect of the laminate by inducing interfacial tensile stresses perpendicular to the FRP laminate.

To evaluate this latter debonding mechanism, several models can be found in the literature (fib 2001; Matthys 2000). As these methods result in a rather complex calculation of the resisting shear force, an alternative Eq. 16.6 is proposed in (Matthys 2000):

$$V_{Rp} = \tau_{Rp} bd \quad (16.6)$$

$$\tau_{Rp} = 0.38 + 151 \rho_{eq} \quad \text{with} \quad \rho_{eq} = \rho_s + \rho_f \frac{E_f}{E_s} \quad (16.7)$$

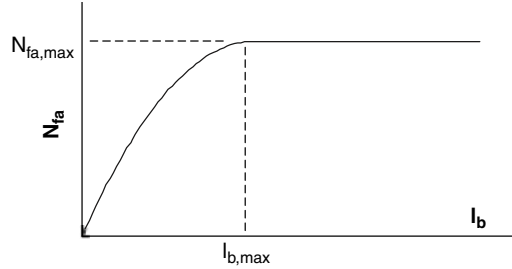
with E the FRP's Young modulus and ρ the reinforcement ratio of the FRP reinforcement (subscript f) and the longitudinal reinforcement (subscript s).

This equation is calibrated on experimental results obtained from 4-point bending tests for concrete strengths C25/30 and C30/37. Both CFRP prefab and wet lay-up types are considered.

16.3.2 Curtailment and Anchorage Length Failure

Theoretically the FRP reinforcement can be curtailed when the axial tensile force can be carried by the internal steel only. The remaining force in the FRP at this point needs to be anchored. Nevertheless, the FRP may need to be extended to zones corresponding to even lower FRP tensile stresses, as the anchorage capacity of the interface is limited (see Fig. 16.6).

Fig. 16.6 Maximum FRP force which can be anchored in function of the bond length



Based on fracture mechanics considerations (Holzenkämpfer 1994), the values of the maximum FRP force which can be anchored, $N_{fa,max}$, and the maximum anchorage length, $l_{b,max}$ (as can be noticed in Fig. 16.6) can be calculated from (fib 2001):

$$N_{fa,max} = \alpha \cdot c_1 \cdot k_c \cdot k_b \cdot b_f \cdot \sqrt{E_f \cdot t_f \cdot f_{ctm}} \quad (16.8)$$

$$l_{b,max} = \sqrt{\frac{E_f \cdot t_f}{c_2 \cdot f_{ctm}}} \quad (16.9)$$

In this equation the geometry of the FRP strip is incorporated in the thickness t_f and the width b_f . Furthermore, α is a reduction factor, approximately equal to 0.9, to account for the influence of inclined cracks on the bond strength; k_c is a factor accounting for the state of compacting of concrete and k_b is a geometrical factor.

16.3.3 End Shear Failure

By curtailing a laminate at a certain distance from a support, a shear crack can appear at the FRP-end. The propagation of this crack is hindered by the internal steel reinforcement (both the stirrups and the longitudinal reinforcement) and the aggregate interlocking. Although, due to the lack of internal steel stirrups between the internal steel reinforcement and the external FRP reinforcement (see Fig. 16.7), this shear crack may propagate as a debonding failure at the level of the internal steel reinforcement. In this case the laminate as well as a thick layer of concrete will rip off.

An important parameter in the mechanism of concrete rip-off is the distance between the plate end and the support. Related to continuous beams, the latter has to be seen as the distance between the plate end and the point of contraflexure.

Based on the concept of the fictitious shear force zone a_L (Fig. 16.8), it is possible to estimate the resisting shear force at the location of the plate end (fib 2001):

Fig. 16.7 Truss system in order to explain the tie initiation of concrete rip-off

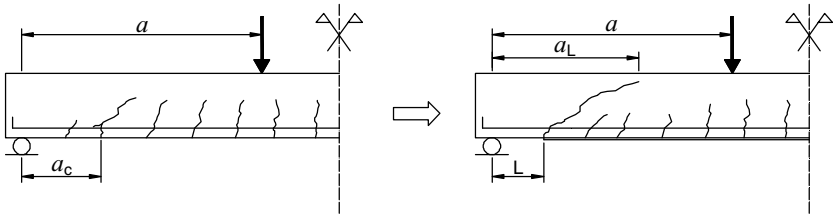
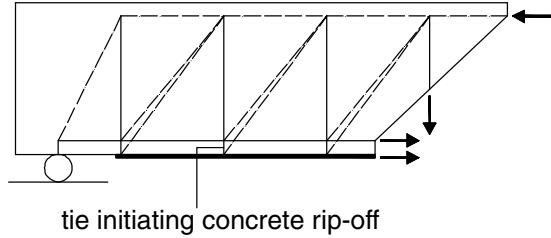


Fig. 16.8 Checking of concrete rip-off

$$a_L = \sqrt[4]{\frac{(1 - \sqrt{\rho_s})^2}{\rho_s}} L^3 d \tag{16.10}$$

$$V_{Rd} = \tau_{Rd} b d \tag{16.11}$$

with τ_{Rd1} the design value of the nominal maximum shear stress.

In these equations only the internal reinforcement is taken into account. Moreover, it has to be mentioned that the model is applicable only if the following conditions are fulfilled $a > L + d$ and $a_L < a$. From experimental research it can be concluded that this model is an accurate lower bound limit for the prediction of concrete rip-off.

16.3.4 Failure Modes in Case of Continuous Beams

By investigating the above-mentioned mechanisms in continuous beams, certain differences with isostatic beams have to be mentioned. A first aspect which may influence the debonding mechanisms in continuous RC beams is that moments of opposite signs occur along the beam. In contrast to reinforced isostatic beams, this allows to anchor the FRP laminates in compression zones. By extending a laminate into these compression zones, two out of the four debonding mechanisms will be avoided: debonding by a limited anchorage length and debonding by end shear failure (concrete rip-off). Care should be taken to limit the length along which the laminate is extended in the compression zone, so as to restrict the compressive stress in the laminate and reduce the chance of local laminate buckling.

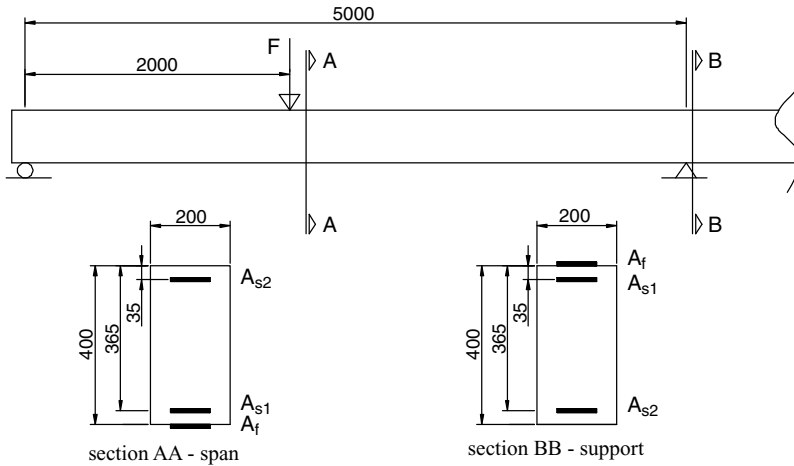


Fig. 16.9 Indication of reinforcement position at critical sections

16.4 Tests on Continuous Beams

16.4.1 Beam Characteristics

For the experimental study of CFRP strengthened continuous beams, three different full-scale 2-span beams were tested up to failure, each with a specific internal steel configuration (Fig. 16.9). Despite the different internal and external reinforcement configurations, a similar failure load is obtained for all beams.

The total depth of the tested beams equals 400 mm, the width equals 200 mm and the span length equals 5 m. The beams are loaded with one point load in each span. The locations of the point loads are at a distance of 3 m from the mid-support and at 2 m from the end supports. Hence $\lambda = 2/3$ (referring to Eq. 16.2). This test set-up is equal to the beam configuration used in the theoretical approach (see Sect. 16.2). The reinforcement ratios according to Eq. 16.7 are given in Table 16.1. As external reinforcement, CFRP laminates with section 100 mm \times 1.0 mm are applied in the zones with low internal reinforcement sections.

Beam CB1 is reinforced with a small amount of internal reinforcement in the spans and a large amount at the mid-support. To compensate the small amount in the spans, externally bonded reinforcement (EBR) is applied only in the spans. A second beam (CB2) has a large amount of internal reinforcement in the spans and a small amount at the mid-support (opposite to CB1). As external reinforcement, EBR is only applied at the top of the beam above the mid-support. The third beam (CB3) has internal reinforcement based on the linear elastic theory. In this case almost the same amount of internal reinforcement is used in the spans and the mid-support. As external reinforcement, laminates are glued on top of the beam above the mid-support as well as at the soffit of the beam in the spans.

Table 16.1 Reinforcement ratios used at mid-support and span [in%]

	Mid-support			Span		
	$\rho_{sup,s}$	$\rho_{sup,f}$	$\rho_{sup,eq}$	$\rho_{span,s}$	$\rho_{span,f}$	$\rho_{span,eq}$
CB1	1.43	–	1.43	0.53	0.13	0.65
CB2	0.31	0.13	0.43	0.75	–	0.75
CB3	0.67	0.13	0.79	0.75	0.13	0.87

Table 16.2 Material properties

	Concrete	Reinforcement span	Reinforcement support	CFRP
f_c (MPa)	38.0	–	–	–
Yield stress (MPa)	–	601	530	–
Yield strain	–	0.28%	0.25%	–
f_{ct} (MPa)	3.4	677	701	2,770
Failure strain	0.35%	12.4%	12.4%	1.46%
E -modulus (GPa)	35.5	218	216	190

The same concrete composition was used for the different beams. A cement type CEM I 52,5 N (300 kg/m³), a sand 0/5 (655 kg/m³), two gravel types 2/8 (190 kg/m³) and 8/16 (1,120 kg/m³) and 165 l of water was used. The main material properties of the concrete, the reinforcing steel and the CFRP laminates are given in Table 16.2.

16.4.2 Test Results

In Fig. 16.10, the experimental and analytical moment redistributions of CB1 are compared. Regarding the unstrengthened beam (dashed line), the formation of a plastic hinge can be noticed (vertical part of the moment distribution curve). In case of the strengthened beam, although the strengthened spans still start to yield first, the FRP allows the spans to continue resisting the additional load and a so-called restrained hinge is formed. The internal restrain is due to the fact that the CFRP laminate shows an elastic behaviour. At increasing load, when the mid-support starts to yield, a plastic hinge occurs at the mid-support.

Shortly after this plastic hinge formation, debonding of one of the span laminates occurred at 153 kN. Good agreement is observed between the experimental curve and the calculated curve.

The experimental and analytical moment redistributions of CB2 are compared in Fig. 16.11. For the unstrengthened beam, the formation of a plastic hinge can be noticed at the mid-support (vertical part of the dashed moment distribution curve). In case of the strengthened beam, although the strengthened mid-support section still starts to yield first (as mentioned above), the FRP allows the mid-support to continue resisting the additional load (restrained hinge formation). At increasing load, when the spans start to yield, a plastic hinge is formed in the spans. At a slightly higher load, the laminate debonded at 152 kN.

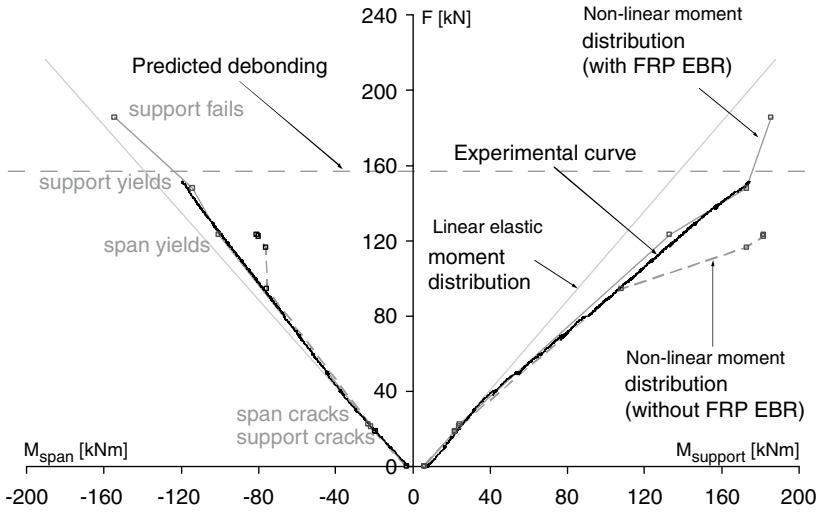


Fig. 16.10 Moment redistribution of beam CB1

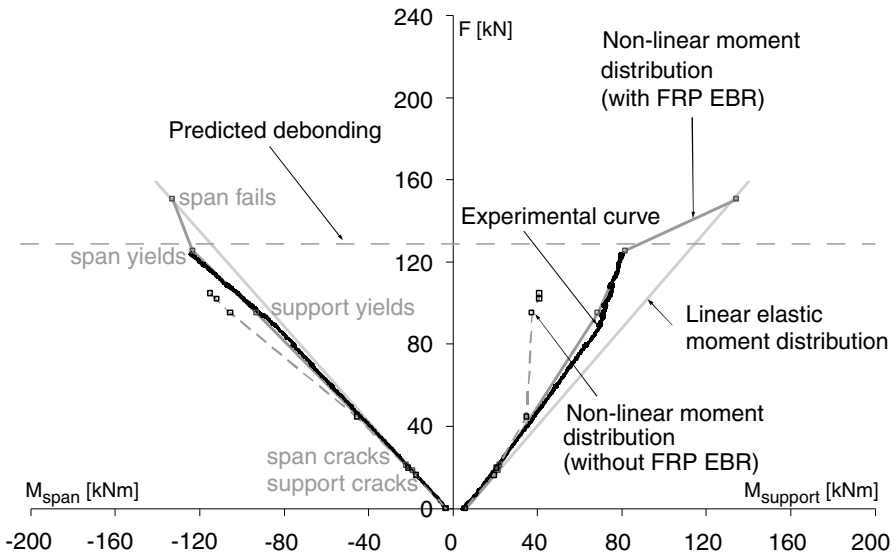


Fig. 16.11 Moment redistribution of beam CB2

Unfortunately no information about the moment redistribution for $F > 122$ kN is available, due to a technical problem by which the signals from the load cells were not recorded beyond 122 kN. Concerning the available experimental data, a good agreement is observed with the calculated curve.

In Fig. 16.12, the experimental and analytical moment redistributions of CB3 are compared. Both for the unstrengthened and for the strengthened beam a moment

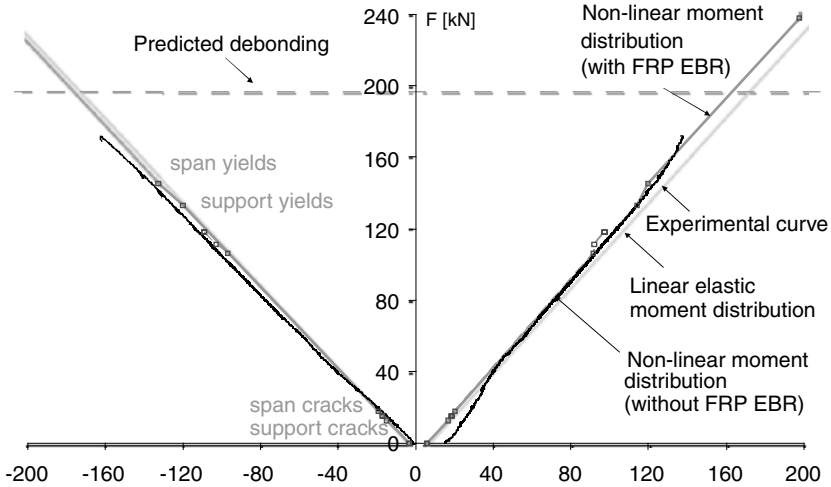


Fig. 16.12 Moment redistribution of beam CB3

distribution is observed similar to the distribution obtained from the linear elastic theory. At increasing load, when the spans and mid-support sections start to yield, the FRP allows both the spans and the mid-support to continue resisting the additional load (restrained hinge formation).

Concerning the available experimental data, a good agreement is observed with the calculated curve. Debonding of the laminate occurs at 170 kN, after both mid-support and spans already yield.

16.5 Conclusions

The use of EBR to strengthen reinforced concrete structures implies the possible occurrence of debonding of the laminates. In the design of a strengthened member, often full composite action is assumed to start with. In a second stage, different debonding mechanisms are considered or verified in the design. The different debonding mechanisms which can appear in the strengthened regions of a continuous beam are similar to the mechanisms which appear in isostatic beams. However, with proper design end shear failure and anchorage failure can be avoided.

In unstrengthened 2-span beams, plastic hinges are expected in the zones with low internal reinforcement ratios (compared to the linear elastic reinforcement ratios). By strengthening only these zones with FRP EBR, the possibility exists to move the location of the plastic hinge to the zones with high internal reinforcement ratios (compared to the linear elastic reinforcement ratios).

The analytically obtained moment redistribution based on a non-linear analysis, shows good to excellent agreement with the experimentally obtained moment redistribution.

The models allow prediction of the debonding failure load with a fairly high accuracy.

Acknowledgements The authors would like to thank the Fund for Scientific Research in Flanders (FWO) for the financial support.

References

- ACI (2002) Guide for the design and construction of externally bonded FRP systems for strengthening concrete structures, ACI 440.2R-02. American Concrete Institute, Farmington Hills
- Chen JF, Yuan H, Teng JG (2007) Debonding failure along a softening FRP-to concrete interface between two adjacent cracks in concrete members. *Eng Struct* 29(2):259–270
- fib (2001) Externally bonded FRP reinforcement for RC structures. International federation for structural concrete. fib bulletin 14, Lausanne, 138 pp
- Matthys S (2000) Structural behaviour and design of concrete members strengthened with externally bonded FRP reinforcement. PhD thesis, Department of Structural Engineering, Ghent University, Ghent, p 345
- Nanni A (1993) Fibre-Reinforced-Plastic (FRP) reinforcement for concrete structures: properties and applications, vol 42. Developments in Civil Engineering, Amsterdam, 450 pp
- NBN-EN-1504-5 (2005) Products and systems for the protection and repair of concrete structures – definitions, requirements, quality control and evaluation of conformity – part 5: concrete injection = EN 1504-5:2004
- Oller E, Cobo D, Mari AR (2007) A new design proposal to prevent failure in beams strengthened by plate debonding. Proceedings, 8th international symposium on fibre reinforced polymer reinforcement for concrete structures (FRPRCS-8), Patras, July 2007
- Teng JG et al (2003) Intermediate crack-induced debonding in RC beams and slabs. *Constr Build Mater* 17(6–7):447–462